UNITED NATIONS UNIVERSITY
UNU-GTP
Geothermal Training Programme

Orkustofnun, Grensasvegur 9,
IS-108 Reykjavik, Iceland

Reports 2014
Number 19

GEOCHEMICAL INTERPRETATION OF DISCHARGE FROM REYKJANES WELLS RN-29 AND RN-32, SW-ICELAND

Melese Mekonnen Berehannu
Geological Survey of Ethiopia
Addis Ababa
P.O. Box 40069
ETHIOPIA
melese147@gmail.com

ABSTRACT

In this report, chemically analysed data from Reykjanes wells RN-29 and RN-32 are used to compare the aquifer temperatures of these wells using selected chemical geothermometers. Calcite and amorphous silica scaling potential is assessed for selected wells. The downhole temperature measurements, the intersection of anhydrite, wairakite, epidote, prehnite and quartz mineral saturation indices and quartz geothermometer results are used to predict the reservoir temperature. From these parameters, the reservoir temperature of Reykjanes well RN-29 is considered to be around 290°C. Similarly, for Reykjanes well RN-32 the reservoir temperature is considered to be around 250°C. The speciation program WATCH was used to calculate amorphous silica and calcite saturation for variably boiled well water. The chemical composition of the fluids was compared with that of a standard sea water composition and the results had the same composition in chloride and total dissolved solids. Reykjanes well RN-29 is assumed to be an excess enthalpy well. The deep liquid composition was computed by a phase segregation model and the results showed that the composition was quite different for volatile components, while the change was insignificant for non-volatile components. Reykjanes well RN-32 was assumed to have a liquid enthalpy in order to compute the deep fluid composition at 250°C reservoir temperature.

1. INTRODUCTION

The Reykjanes geothermal system is located on the southwest tip of the Reykjanes Peninsula in SW-Iceland (Figure 1). The geothermal surface manifestations at Reykjanes include altered rocks, steam vents, mud pits and warm ground (Fridriksson et al., 2006). The reservoir fluid in the Reykjanes system is hydrothermally modified seawater with some addition of magmatic gases (Arnórsson, 1978; Ólafsson and Riley, 1978; Freedman et al., 2010; Hardardóttir et al., 2009; Óskarsson et al., 2014). In Section 2 of this study, a general background of the Reykjanes field is provided: geological and structural setting, chemical studies of the area are described, and the drilling operations for wells RN-29 and RN-32 reviewed. In Section 3, the sampling and analysis of geothermal fluids is described, including fluid classification, geothermometers, and solution mineral equilibria. In this study, the chemically analysed data for Reykjanes wells RN-29 and RN-32 were used to evaluate deep fluid composition, solution mineral equilibria and to estimate subsurface temperatures in the geothermal systems. The subsurface

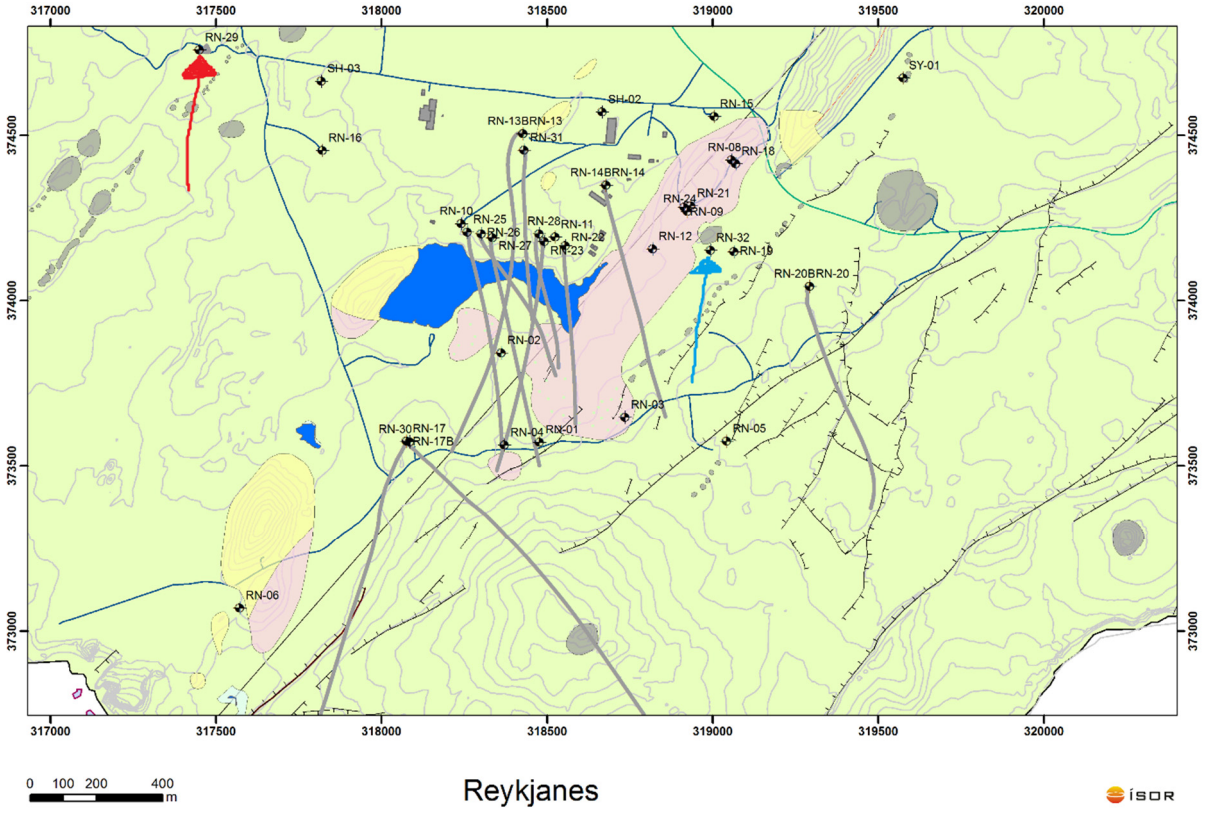

FIGURE 1: Location of wells RN-29 (in red) and RN-32 (in blue) at Reykjanes shown on a map showing surface topography, surface structural features and geothermal manifestations (from K. Saemundsson, pers. comm., revised maps)

temperatures predicted by various geothermometers are compared with measured (downhole) temperatures. Calculations of deep fluid composition were performed with the WATCH speciation program version 2.4 (Bjarnason, 2010). The enthalpy of the discharge from well RN-32 is similar to that of steam saturated water at the aquifer temperature. The enthalpy of the discharge from well RN-29 is higher than that of liquid water at the aquifer temperature. An attempt is made to apply and explore the sensitivity of calculated aquifer fluid composition to assumed phase segregation pressure for well RN-29. The state of chemical equilibria between the main hydrothermal alteration minerals and solutions of the gaseous components will be assessed. In Section 4, the deep fluid composition calculated with WATCH speciation program version 2.4 (Bjarnason, 2010), based on modelled liquid enthalpy and excess enthalpy, is provided. In Section 5, the results obtained from the modelling described in Section 4 are presented and discussed. In addition to assessing the state of equilibria with respect to mineral-solution and mineral-gas reactions, the change in chemical composition, fluid classification, geothermometers and production properties are described in this section. In Section 6, conclusions and directions for future work are presented and discussed.

2. REYKJANES GEOTHERMAL FIELD

2.1 Geological and structural setting

The Reykjanes geothermal system consists of young, highly permeable basaltic formations, transsected by an intense NE-SW trending fault zone, and is tectonically active (Björnsson et al., 1970). The volcanic activity on the Reykjanes peninsula is concentrated along five distinct fissure swarms, but central volcanic complexes are notably absent at the four westernmost ones (Jakobsson et al., 1978).

The volcanic rocks are of basaltic composition ranging from picrite shield lavas through olivine tholeiite shield lavas and fissure products; no intermediate or rhyolitic rocks crop out west of the Hengill central volcano (Jakobsson et al., 1978). High temperature geothermal systems are found in all Reykjanes Peninsula fissure swarms. The Reykjanes geothermal area is located at the centre of swarms of active faults that facilitate hydrologic convection. High-level magma chambers have apparently not formed in the Reykjanes volcanic systems (Gudmundsson and Thórhallsson, 1986), and sheeted dike complexes are likely to serve as the magmatic heat source for the geothermal activity. Surface geothermal manifestations occur over an area of ~1 km^2, but observations from more than 30 drillholes and several resistivity surveys indicate that the subsurface area of the active system is at least 2 km^2, consistent with the findings of Björnsson et al. (1972) and Pálmason et al. (1985).

2.2 Geochemical studies

The Reykjanes geothermal water represents heated seawater with freshwater mixing (Ólafsson and Riley, 1978). However, fluid inclusion studies on borehole cuttings and stable isotope ratios of geothermal fluids and secondary minerals indicate that dilute fluids dominated the system at earlier times (Sveinbjörnsdóttir et al., 1986; Franzson et al., 2002; Pope et al., 2010). The difference in the composition of seawater and the geothermal water is due to interaction with the basaltic host rocks at elevated temperatures, with the geothermal water enriched in SiO_2, K, Ca and depleted in SO_4 and Mg but with the same Cl concentration as the seawater (Björnsson et al., 1970, 1972; Arnórsson, 1978, 1983). The Reykjanes geothermal system has been identified as an active ore-forming system (Hardardóttir et al., 2001). Scales enriched in metals are common in pipelines at Reykjanes and they include the minerals sphalerite, bornite, digenite, galena, chalcopyrite, native silver, silver sulphides, gold (probably occurring in solid solutions or as submicroscopic inclusions) and pyrite among others, with abundances varying from well to well due to differences in the physical parameters of the wells (Hardardóttir et al., 2009). The Reykjanes geothermal system is surrounded by the ocean on three sides, only 1.5 km from the shoreline and extends southwest to the sea (Björnsson et al., 1971; Gudmundsson et al., 1981; Johnsson and Jakobsson, 1985).

2.3 Wells RN-29 and RN-32

The drilling operations at well RN-29 at Reykjanes were carried out by Iceland Drilling Co. for HS Orka, the operator of the field. Well RN-29 is a vertical well. The location of well RN-29 is shown in Figure 1. The drilling of the first stage was completed on April 7th 2010 at 306 m depth, and the second stage ended on April 29th at 902 m depth, and the third and the last stage of drilling was completed on June 8th at 2837 m. Samples of drill cuttings were collected at 2 m intervals and lithological and alteration analyses were carried out during the course of drilling. Well RN-29 intersects several hyaloclastite formations made from tuffs, tuffaceous sediments, breccias and pillow basalts. A few lava series were found in between hyaloclastite units. Holocene lavas and tephra units are at the surface. Around 40 basalt intrusions were identified, 17 of which are thicker than 10 m. The drilling of well RN-32 at Reykjanes was commissioned by HS Orka. Well RN-32 is designed as a production well and was drilled as a make-up well to provide steam to maintain 100 MWe generation in the Reykjanes power plant. The location of well RN-32 is shown in Figure 1. The well was drilled in 3 stages. The drilling of the first stage was completed on February 14th 2013 at 350 m depth, and the second stage ended on April 5th at 1080 m depth. The third and last stage of drilling was completed on April 16th at 1202 m. Well RN-32 goes through several hyaloclastite formations, made from Holocene lava, basaltic tuffs, basaltic breccias, fine- and medium-grained basalt and tuff rich sediments (Gunnarsdóttir et al., 2013).

3. CHEMISTRY OF GEOTHERMAL FLUIDS

3.1 Sampling and analysis of geothermal fluids

The collection of representative samples from discharging wells involves separate collection of the steam phase and the water phase. This is done with the aid of a Webre separator and a cooling device. Great care must be taken to separate steam completely from the liquid. The separator is connected to the steam line and kept open to rinse and warm it up for at least 10 min. Then it is closed and the sampling pressure (Ps) is recorded from the pressure gauge installed on the separator. The geothermal fluids are separated completely in order to discharge steam through the steam outlet, and liquid through the liquid outlet; each is rinsed for a few minutes before sampling. The condensed steam and the non-condensable gases are then collected into an evacuated double port bottle containing a concentrated solution of NaOH (40 wt%). The most abundant gases, CO_2 and H_2S, will dissolve in the caustic solution and the other gases will be collected in the head space. Figure 2 is a schematic diagram of the sampling procedure for geothermal wells.

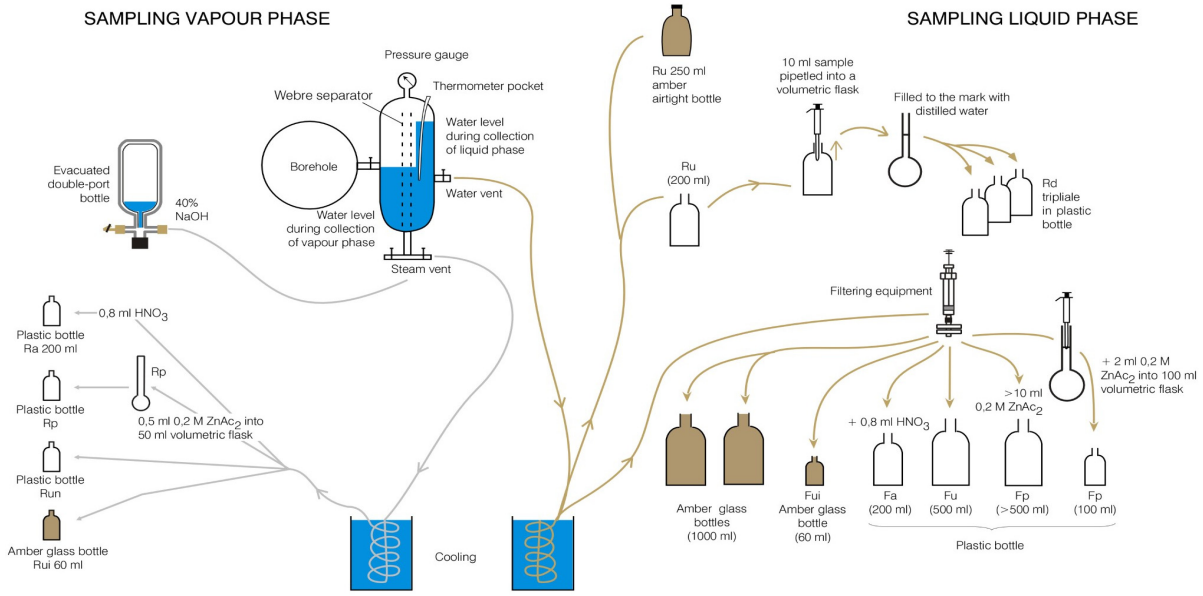

FIGURE 2: Collection of sample from a two-phase geothermal well for chemical analysis (from Ármannsson and Ólafsson, 2006)

Chemical analysis of geothermal water samples must meet certain levels of accuracy and reliability to be useful in identifying geochemical processes in hydrothermal systems. Quality control is largely a concern for the analytical laboratory, but the geochemist using the chemical data must also be concerned with analytical quality. Chemical analyses were examined for internal consistency by calculating the error in the ionic charge balance. To be considered internally consistent, chemical analyses must have less than 5% error in the charge balance. In this study, the geothermal water samples are from Reykjanes wells RN-29 and RN-32, and were collected in 2011 and 2014. All the sampling and analyses were carried out by ISOR (Iceland GeoSurvey). After collection, the samples were treated. A summary of the sample preparation methods is presented in Table 1. The analytical methods used are listed in Table 2. The results of the analyses is are in Table 3. The charge balance error, which is reported in Table 3, is calculated by Equation 1:

$$CBE(\%) = \frac{\sum ZcatMcat - \sum ZanMan}{\sum ZcatMcat + \sum ZanMan} x100\% \quad (1)$$

where Z_i = Charge of an ion
M_i = Molar concentration of i (mol/Kg)

TABLE 1: Sample preparation methods

Treatment	Container	Specification	To determine
None; amber glass bottle with ground glass Stopper	250-300 ml glass	Ru (Rw, untreated)	pH, CO_2, NH_4, H_2S (if not in field), conductivity
Dilution; 5 ml of sample added to 45 ml of distilled, deionised water	3 x 100 ml plastic	Rd (raw, diluted) (1:10)	SiO_2 if > 100 ppm
Filtration	200 ml plastic	Fu (filtered, untreated)	Anions
Filtration; 0.8 ml conc. HNO_3 added to 200 ml sample	200 ml plastic	Fa (filtered, acidified)	Cations
Filtration; 2 ml 0.2 M $ZnAc_2$ added to sample in 100 ml volumetric glass flask to precipitate sulphide	100 ml, plastic	Fa (Filtered, acidified)	SO_4

TABLE 2: The analytical methods employed at Iceland GeoSurvey

Constituent	Fraction	Method
pH	Ru	pH-meter
CO_2	Ru	Electrometric titration
H_2S	Ru	Titrimetric method
NH_4	Ru	Spectrophotometry
SiO_2	Rd	Spectrophotometry
F	Fu	Selective electrode
Cl	Fu	Ion chromatography
SO_4	Fp	Ion chromatography
B	Fu	Spectrophotometry
Na	Fa	Atomic absorption spectroscopy – direct aspiration
K	Fa	Atomic absorption spectroscopy – direct aspiration
Mg	Fa	Atomic absorption spectroscopy – direct aspiration
Ca	Fa	Atomic absorption spectroscopy – direct aspiration
Al	Fa	Atomic absorption spectroscopy – graphite furnace
Fe	Fa	Atomic absorption spectroscopy – graphite furnace
TDS	Fu	Gravimetric
H_2, N_2, O_2, Ar, CH_4	Gas bulb	Gas chromatography

TABLE 3: Measured discharge enthalpies, sampling pressures and analysis of major elements

LIQUID PHASE (mg/kg)

Well no.	Sample ID	SP (bar-g)	H (kJ/kg)	pH/°C	CO_2	H_2S	NH_3	B	SiO_2	Na	K	Mg	Ca	F	Cl	SO_4	Al	Fe	TDS	CBE (%)
RN-29	20140009	17.5	2250	5.15/22.5	45.5	1.44	2.06	13.1	1088	14630	2520	2.86	1950	0.27	28600	16.3	0.022	3.82	49880	-0.46
RN-29	20110005	16.5	1880	5.57/21.6	25.5	2.58	1.58	9.54	953	12320	2150	1.44	1580	0.24	24100	20.9	0.0277	0.901	41270	-0.71
RN-32	20140137	15.7	1029	6.37/22,1	10	0.27	1.3	7.99	649	10250	1490	1.14	1520	0.22	19950	27.1	0.128	0.485	34430	-0.27

VAPOUR PHASE (mg/Kg)

Well no.	Sample ID	CO_2	H_2S	H_2	O_2	N_2	CH_4	NH_3
RN-29	20140009	11000	840	7.86	0.01	85.4	1.5	3.32
RN-29	20110005	8530	300	0.73	91.8	935	0.53	2.35
RN-32	20140137	660	32	0.25	0.01	34.3	0.03	3.97

TDS - Total dissolved solids CBE - Charge balance error
SP - Sampling pressure

3.1 Fluid classification

The most common type of fluid found at depth in high-temperature geothermal systems is of near-neutral pH, with chloride as the dominant anion. Other waters encountered in geothermal areas are commonly derived from this deep fluid as a consequence of chemical or physical processes. These waters, the characteristics of which are described below, are classified according to the dominant anions:

1) Chloride water type in which the chloride is the dominant anion and often attains concentrations in the thousands of mg/kg range.
2) Sulphate type water also known as acid-sulphate waters: these are invariably surface fluids formed by the condensation of geothermal gases into near surface, oxygenated groundwater.
3) Bicarbonate waters, which include those termed CO_2-rich fluids and neutral bicarbonate-sulphate waters, are the product of steam and gas condensation into poorly-oxygenated sub-surface ground waters.
4) Sulphate-chloride waters can form by several processes, and the following have been suggested: the mixing of chloride and sulphate waters at variable depths; near-surface condensation of volcanic gases into meteoric waters; and condensation of magmatic vapour at depth.

Most geochemical techniques may, with confidence, be applied only to specified types of fluids with limited ranges of composition. Any such interpretation of geothermal water samples, therefore, is best carried out on the basis of an initial classification. The Cl – SO_4 – HCO_3 ternary diagram is one of the diagrams for the classification of natural waters (Giggenbach, 1991). The position of a data point in such a triangular plot is obtained by first calculating the sum S of the concentrations C_i (mg/kg) of all three constituents involved:

$$S = C_{Cl} + C_{SO4} + C_{HCO3} \tag{2}$$

Once the sum percentages of Cl, SO_4 and HCO_3 are obtained, then D = HCO_3 % + 0.5Cl % is computed. The Cl % and D are plotted as Y and X axes, respectively. In this diagram, composition ranges are indicated for several typical groups of water such as volcanic and steam-heated waters, mature waters and peripheral waters. The triangular Cl – SO_4 – HCO_3 diagram can be used to classify the geothermal waters, especially, and to filter out waters for geochemical techniques (Giggenbach, 1988).

Giggenbach (1988) pioneered techniques for the derivation of Na–K-Mg-Ca geoindicators. If only Na-K-Mg are considered, a triangular diagram can be used to distinguish between equilibrated, partially equilibrated and immature waters. Geothermometers can only be applied to equilibrated and partially equilibrated waters. The triangular diagram is based on the temperature dependence of the two reactions:

$$K - feldspar + Na^+ = Na - feldspar + K^+ \tag{3}$$

$$2.8\,K - feldspar + 1.6\,water + Mg^{2+} = 0.8\,K - mica + 0.2\,chlorite + 5.4\,silica + 2K^+ \tag{4}$$

The position of a data point in the triangular plot is first used to obtain the sum *S* of the concentrations of *C* (in mg/kg) of all three constituents involved, as in the previous case; only individual constituents are manipulated differently.

$$S = C_{Na}/1000 + C_K/100 + \sqrt{C_{Mg}} \tag{5}$$

From the sum (*S*), C_{Na}/1000% and $\sqrt{C_{Mg}}$% are obtained, then D = $\sqrt{C_{Mg}}$% + 0.5 C_{Na}/1000 % is computed. The Na% and D are plotted as Y and X axes, respectively. The area of partial equilibrium suggests either a mineral that has dissolved but has not attained equilibrium, or a water mixture that has reached equilibrium. A point close to the √Mg corner usually suggests a high proportion of relatively cold ground water, not necessarily "immature".

3.2 Geothermometers

Geothermometers may be used to estimate the temperature of the reservoir fluid. They are valuable tools in the evaluation of new fields, and in monitoring the hydrology of systems in production.

Geothermometers are based on one or more constituents in geothermal fluids (either solutes or gases, and may include isotopes of elements) of which concentrations or proportions in a fluid are controlled, primarily by the temperature of the fluid and the surrounding rock. Many are based on particular chemical equilibrium reactions. Geothermometers can be applied to well or natural surface discharges to obtain approximate subsurface temperatures. The most important water geothermometers are silica (quartz and chalcedony), Na/K ratio and Na-K-Ca geothermometers. Others are based on cation ratios and any uncharged aqueous species, as long as equilibrium prevails (Arnórsson and Svavarsson, 1985). A temperature equation for a specific equilibrium constant refers to a specific mineral-solution reaction. Silica geothermometers are based on experimentally determined variations in the solubility of different silica species in water, as a function of temperature and pressure (e.g. Fournier, 1977). The basic reaction for silica dissolution is:

$$SiO_2(qtz) + 2H_2O = H_4SiO_4 \quad (6)$$

In most geothermal systems, deep fluids at temperatures >180°C are in equilibrium with quartz; it is stable up to 870°C and has the lowest solubility compared to other silica polymorphs. Quartz is common as a primary and secondary (hydrothermal) rock- forming mineral. Silica polymorphs with a less ordered crystal structure (i.e. chalcedony, opal, cristobalite) have higher solubilities than quartz and primarily form at temperatures lower than 180°C. The calibration used here to calculate quartz temperature is (Fournier, 1977):

$$T = 1309/(5.19 - logS) - 273.15 \quad (Quartz - no\ steam\ loss) \quad (7)$$

Here S represents silica concentration as SiO_2 in mg/kg and T is temperature (°C). The quartz geothermometer is best for reservoir conditions >150°C. Below this temperature chalcedony, rather than quartz, probably controls the dissolved silica content. The Na/K geothermometer has steadily evolved over the past thirty years from the initial observation that low Na/K ratios were indicative of high temperature at depth, to increasingly more precise calibration of the temperature dependence of this ratio. In high-temperature systems, the temperature dependant variation of sodium and potassium in geothermal waters is due to ion exchange of these elements between co-existing alkali feldspars according to the reaction:

$$Na - feldspar + K^+(aq) = K - feldspar + Na^+(aq) \quad (8)$$

Chloride waters from high-temperature reservoirs (≥180°C) are suitable for this geothermometer. For lower temperature reservoirs where fluids have long residence times, the Na-K geothermometer may, in some cases, be applicable. The calibrations used in this study are:

Fournier, 1979:

$$T = 1217/(1.483 + \log\left(\frac{Na}{K}\right)) - 273.15$$

Giggenbach, 1988:

$$T = 1390/(1.75 + \log(\frac{Na}{K})) - 273.15$$

Arnórsson, 1983 (250-350°C):

$$T = 1319/\left(1.699 + \log\left(\frac{Na}{K}\right)\right) - 273.15$$

One of the advantages of this geothermometer is that it is less affected by dilution or steam loss as it is based on a ratio of concentrations. On the other hand, the Na-K geothermometer sometimes gives poor results below 100°C. It is also unsuitable if the waters contain high concentrations of calcium (Ca), as is the case for springs depositing travertine.

3.3 Solution mineral equilibria

The position of solution mineral equilibria may change as a result of the chemical and physical processes which take place in the geothermal fluid, both in the reservoir and as it ascends to the surface. The chemical processes centre around mineral-fluid reactions, both dissolution and deposition, while the dominant physical process is boiling, although conductive cooling and mixing are also important. Common dissolved constituents in the deep chloride reservoir fluids fall into two groups:

1) Conservative species (Cl, B, Br, As, Cs) which readily pass into solution, often before appreciable alteration of the host rock has occurred, and;
2) Common rock forming species (e.g. SiO_2, Na, K, Ca, Mg etc) whose solubilities are controlled by temperature dependant mineral-fluid equilibria and only enter the solution after alteration of the host minerals.

There are two types of mineral-fluid equilibria which need to be considered: solubility equilibria (e.g. quartz, calcite); and ion-exchange equilibria (e.g. Na and K between feldspars and micas). Solubility reactions determine how much of a particular species can enter or remain in solution before precipitation occurs. Temperature is the dominant control on mineral solubility in geothermal systems, but changes in pH, pressure or salinity can also have an effect. Silica and calcite equilibria are particularly important in geothermal systems, as they govern the amount of SiO_2 and Ca in solution, and are two of the main causes of scaling in wells. The solubility of any silica mineral can be written as:

$$SiO_{2\,(s)} + 2H_2O_{(l)} = H_4SiO_{4(aq)} \quad (9)$$

and the solubility constant is given by:

$$K_{SiO_2} = a_{H_4SiO_4} \quad (10)$$

Silicic acid is a weak acid and dissociates to yield hydrogen ions. If the pH of the solution is increased, that is it becomes more alkaline, then the solubility of silica will also increase as the hydrogen ions are consumed by the reactions:

$$HCO^-_{3(aq)} + H^+_{(aq)} = H_2CO_{3(aq)} = H_2O_{(l)} + CO_{2(g)} \quad (11)$$

Geothermal reservoir fluids are commonly close to saturation with respect to calcite (Arnórsson, 1989). The dissolution of calcite can be expressed by the equation:

$$CaCO_{3(s)} + H_2O_{(l)} + CO_{2(g)} = Ca^{2+}_{(aq)} + 2HCO^-_{3(aq)} \quad (12)$$

Calcite solubility, therefore, increases with increasing P_{CO2} (up to mCO_2 ~ 1 mole/kg, Fournier, 1985).

The lowering of P_{CO_2} upon boiling, as carbon dioxide is lost to the steam phase, increases the pH of the solution and leads to supersaturation and precipitation of calcite. As carbon dioxide has minimum solubility at around 160-180°C, boiling near this temperature can lead to calcite supersaturation. As the temperature of the liquid phase decreases, the solubility of calcite increases. Cooling of a solution, either by boiling or conduction, can lead to greater undersaturation with respect to calcite and other carbonate minerals. Generally, calcite solubility is increased by decreasing temperature, increasing CO_2 partial pressure and increasing salinity.

Ion exchange reactions involve the transfer of ions between two or more alumino-silicate minerals and control the ratios of cations in solution, including H^+. This means that solution pH can be buffered by a silicate mineral assemblage. Observations on geothermal alteration assemblages show that the majority of secondary minerals are formed by reaction such as:

Albite – K-feldspar

$$NaAlSi_3O_{8(s)} + K^+_{(aq)} = KAlSi_3O_{8(s)} + Na^+_{(aq)} \quad (13)$$

$$K = a_{Na}/a_K \quad (14)$$

K-feldspar – K-mica + quartz

$$3KAlSi_3O_{8(s)} + 2H^+_{(aq)} = KAlSi_3O_{10}(OH)_{2(s)} + 6SiO_{(2)} + 2K^+_{(aq)} \quad (15)$$

and $K = a_K/a_H$

Wairakite – Ca-montmorillonite + quartz

$$1.17CaAl_2Si_4O_{12}.2H_2O_{(s)} + 2H^+_{(aq)} = Ca_{0.17}Al_{2.33}Si_{3.7}O_{10}(OH)_{2(S)} + SiO_{2(s)} + 2H_2O_{(l)} + Ca^{2+}_{(aq)} \quad (16)$$

$$K = a_{Ca}/a_{H^2} \quad (17)$$

Reactions also take place between minerals and gases, and the reaction of iron sulphide with hydrogen sulphide illustrates such a mineral-gas buffering reaction:

Pyrite – pyrrhotite

$$FeS_{2(S)} + H_{2(g)} = FeS_{(s)} + H_2S_{(g)} \quad (18)$$

$$K = P_{H_2S}/P_{H_2} \quad (19)$$

4. CALCULATION OF DEEP FLUID COMPOSITION

4.1 The speciation program WATCH

Evaluation of chemical equilibria between minerals and solutions in natural water systems requires the determination of aqueous species activity and the knowledge of the solubility of the minerals found in the altered rocks. The large number of ions, ion pairs and complexes in the solution, particularly at elevated temperatures, requires the use of a computer program for the calculation of individual species activity from analytical data. In this study, the WATCH speciation program version 2.4 (Bjarnason, 2010) was used to calculate the component concentrations in the geothermal reservoir water, based on chemical analysis of water and steam samples collected from discharging wells. In the calculation of aquifer water composition, it is assumed that no transfer of heat or mass occurs on the way from the reservoir to the surface, i.e. the system was assumed to be isolated. The saturation index of secondary and primary minerals is defined by:

$$SI = log\ (Q/K) \quad (20)$$

where K = The equilibrium solubility constant for a particular mineral dissolution reaction; and
Q = The reaction quotient.

The equilibrium mineral-water reactions potentially controlling the geothermal water composition must involve the observed secondary minerals. In this study, the analytical data of samples collected at the wellheads (Table 3) were recalculated to the deep aquifer fluid conditions with the aid of the WATCH speciation program version 2.4 (Bjarnason, 2010). This procedure is relatively simple for wells discharging liquid enthalpy. In this case, the pressure drop induced by discharging the well is not enough to start boiling in the original aquifer fluid. The level of first boiling is within the well and it is reasonable to treat the aquifer and the well as an isolated system and to assume adiabatic boiling of the fluid. The WATCH speciation program calculates individual species activities in the aquifer fluid. This permits derivation of activity products for minerals and, from the solubility constants for these minerals, their state of saturation in the fluid can be obtained.

4.2 Excess enthalpy

If the pressure produced by a discharging well is sufficient to cause extensive boiling in the producing aquifer, it is common for the discharge enthalpy of the well to be significantly higher than the enthalpy of the aquifer fluid beyond the zone of depressurization around the well. The aquifer-well system is no longer isolated. The discharge enthalpy of the well can increase from its initial enthalpy in the aquifer fluid by conductive heat transfer between the aquifer rock and the flowing fluid, which is cooled by depressurization boiling. The aquifer-well is a closed system since there is an exchange of energy with the surrounding rock but the composition of the fluid does not change (model 2 in Arnórsson et al., 2010). Thus, in the isolated and closed systems, the total well discharge composition is equivalent to that of the initial aquifer fluid.

The measured discharge enthalpy for well RN-29 was 2250 kJ/kg in 2014 and 1880 kJ/kg in 2011, but the calculated aquifer fluid discharge enthalpy is 1290 kJ/kg at 290°C. The increase in the enthalpy as the fluid flows from the undisturbed aquifer to the wellhead is primarily due to segregation of the vapour and liquid water in the aquifer. The vapour phase flows to the well head while liquid water is partially or totally retained in the aquifer, adhering onto mineral grain surfaces by capillary forces. The mechanism of phase segregation is, therefore, an open system, causing both the enthalpy and composition of the flowing fluid to change from the initial aquifer conditions to the wellhead (model 3 in Arnórsson et al., 2010).

The deep fluid composition of wells with excess enthalpy may be calculated in two steps using the WATCH program, as explained by Arnórsson et al. (2010). The first step consists of calculating the vapour fraction and the liquid and vapour compositions at the pressure (P_g) at which phase segregation is assumed to occur. For this study, phase segregation pressure or temperature is considered to be 30°C lower than the aquifer temperature of 290°C, which was calculated by geothermometers, i.e. 260°C corresponding to a pressure of 46.9 bar-a. The second step involves calculating aquifer fluid composition from the liquid and vapour phase compositions at P_g, assuming that the flowing fluid enthalpy, before phase segregation occurred, is the same as that of vapour-saturated liquid at the aquifer temperature.

5. RESULTS AND DISCUSSION

5.1 Mineral saturation

The saturation index values are calculated to evaluate with which minerals the fluid is saturated, undersaturated and supersaturated. This was done using the WATCH program, which calculates log$Q$ and log$K$ values for 29 minerals, from which saturation index values are calculated. Figures 3, 4, and 5 show the saturation index values for the minerals anhydrite, wairakite, epidote, prehnite and quartz, all of which are found in drill cuttings from Reykjanes, calculated from deep liquid at different temperatures.

For well RN-29 in 2011, the graph shows that quartz approaches equilibrium at depth and becomes supersaturated through boiling; the solution is supersaturated with respect to prehnite and wairakite at all the temperatures; saturation with anhydrite and epidote appears to be

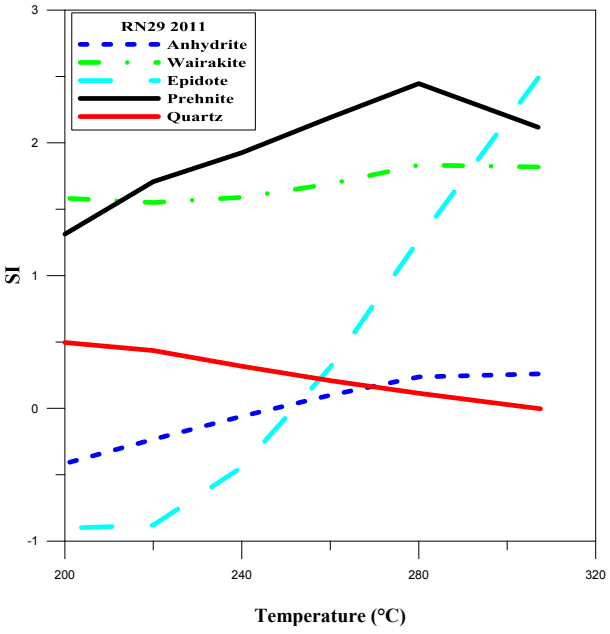

FIGURE 3: Saturation index of selected minerals against temperature for well RN-29 (2011)

temperature-dependent and the solution is supersaturated with respect to them at depth, becoming undersaturated at a lower temperature. The intersection of these mineral curve is assumed to be at the reservoir temperature. For well RN-29 in 2014: the solution similarly remained supersaturated with respect to prehnite and wairakite at all the temperatures; anhydrite and quartz reached equilibrium at a high temperature and the solution became supersaturated with respect to them at a low temperature; similarly, epidote is temperature-dependant and the solution becomes becomes supersaturated with respect to it at a high temperature but undersaturated at a low temperature. The slight difference in the samples was anticipated due to drilling fluid contamination because the RN-29 2011 sample was taken at the end of drilling.

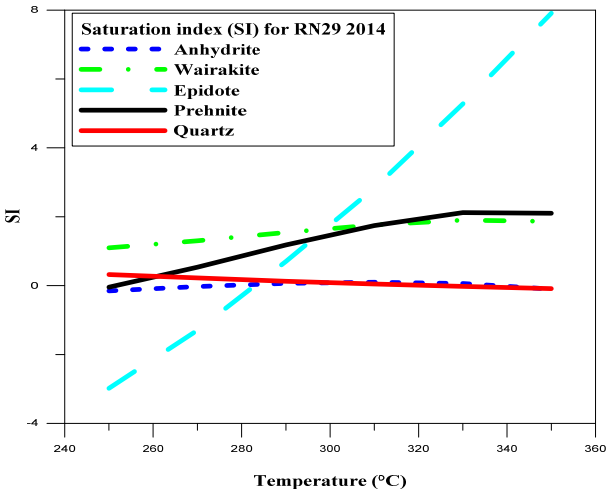

FIGURE 4: Saturation index of selected minerals against temperature for well RN-29 (2014)

For well RN-32 in 2014, the solution was supersaturated with respect to the minerals prehnite, wairakite and epidote were at all temperatures, however, quartz was in equilibrium at high temperatures and the solution became slightly supersaturated with respect to it at a low temperature; it was supersaturated with respect to anhydrite at high temperatures and became undersaturated at a low temperature. The intersection of the anhydrite and quartz curves helped to estimate the reservoir temperature.

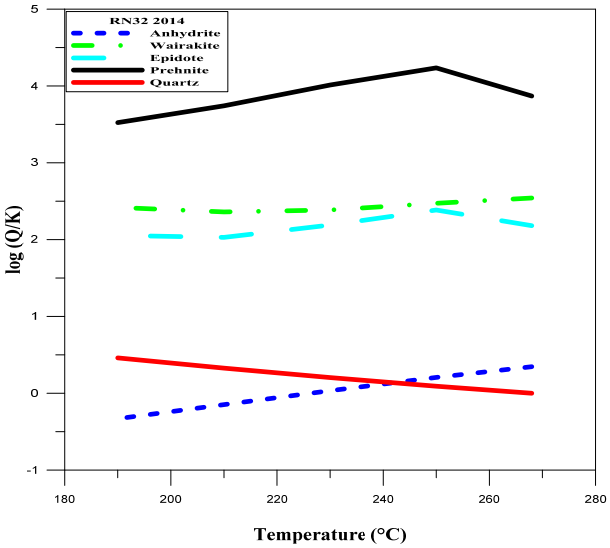

FIGURE 5: Saturation index of selected minerals against temperature for well RN-32

5.2 Geothermometry

The temperature of the reservoir fluid was calculated using various geothermometers, as presented in Table 4. The quartz geothermometer of Fournier (1977) gives higher values in all cases, compared to the sodium/potassium geothermometers. On the other hand, the sodium potassium values calculated from Fournier (1979) and Giggenbach (1988) are very similar, but those calculated from Arnórsson et al.'s (1983) formula gave considerably lower results.

TABLE 4: Geothermometer results

Type of geothermometer	Authors	RN-29 (2014)	RN-29 (2011)	RN-32 (2014)
Quartz	(Fournier, 1977)	334°C	318°C	277°C
Sodium potassium	(Fournier, 1979)	279°C	280°C	261°C
Sodium potassium	(Giggenbach, 1988)	279°C	281°C	264°C
Sodium potassium	(Arnórsson et al.,1983)	266°C	267°C	236°C

The temperature logs show that the feed zone and maximum temperatures are at around 280 and 330°C, respectively, for well RN-29. For well RN-32, the feed zone and maximum temperatures are both at around 250°C.

Based on mineral saturation curve intersections, geothermometers and temperature log values shown in Figure 6, the reservoir temperature is assumed to be 290°C for well RN-29 and 250°C for well RN-32.

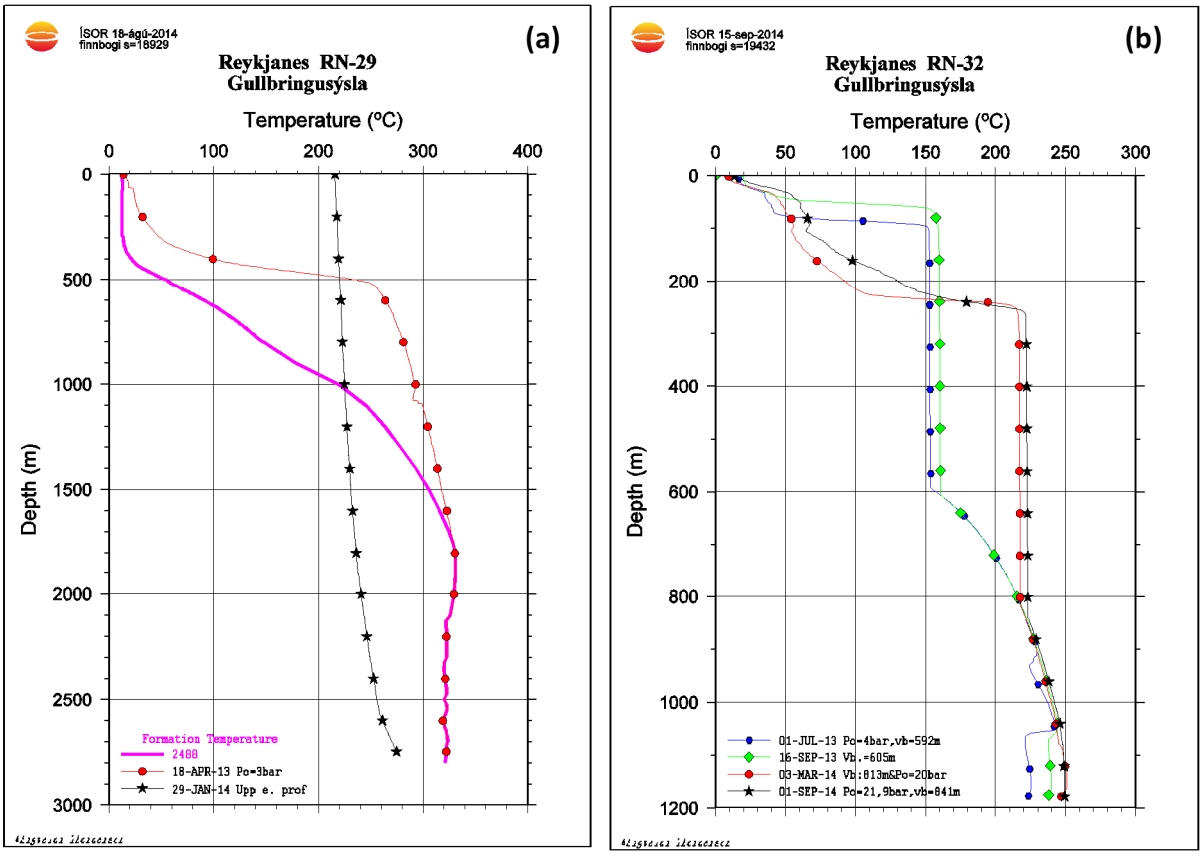

FIGURE 6: Temperature logs for wells RN-29 (a) and RN-32 (b)

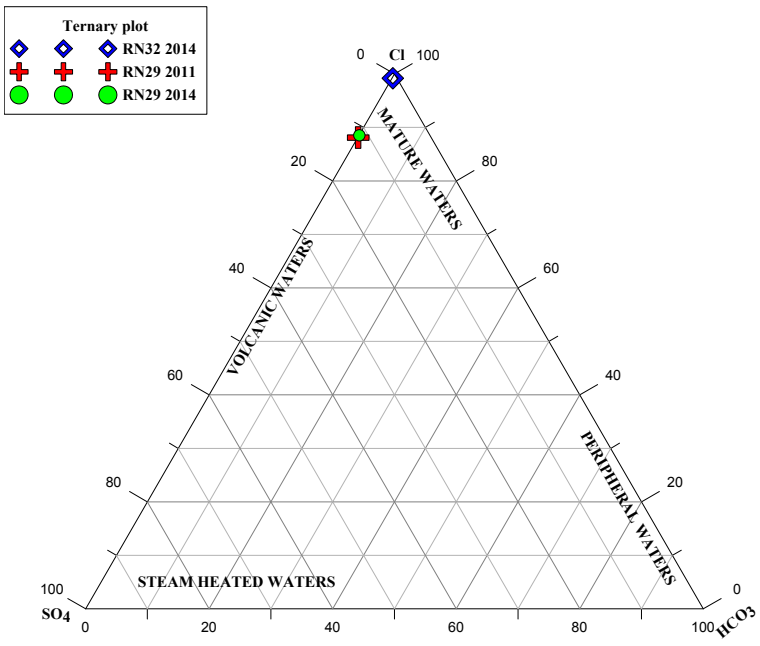

FIGURE 7: Cl-SO_4-HCO_3 ternary diagram

5.3 Ternary diagrams

The Cl-SO_4-HCO_3 ternary diagram is commonly used to classify geothermal waters based on the relative proportions of chloride, sulphate and bicarbonate ions. The diagram indicates several types of thermal fluids such as mature waters, peripheral waters, volcanic, and steam-heated waters. The degree of separation between data points for high chloride and bicarbonate waters gives an idea of the relative degrees of interaction of the CO_2 charged fluids at lower temperatures, and of the HCO_3 contents increasing with time and distance travelled underground. The ternary diagram in Figure 7 shows that the wells fluids from Reykjanes are classified as mature waters. Similarly, the Na-K-Mg ternary diagram shown in Figure 8 indicates that the water is in equilibrium with rock and that the reservoir temperature in the range of 265-290°C.

5.4 Deep fluid composition

The chemical composition of the reservoir water has been calculated from a chemical analysis of water and steam samples collected separately at a known wellhead pressure. The results are presented in Table 5. From the results it may be seen that the concentrations of most of the constituents for well RN-29 are lower in 2011 than in 2014 with the exception of the components SO_4, N_2 and O_2 which have higher concentrations than in 2014. The higher SO_4 concentration and lower H_2S concentration are most likely due to remnants of the fresh water which was used during drilling, but N_2 and O_2 concentrations are due to air contamination of this particular steam sample. Well RN-32 has lower concentrations than well RN-29 in most of the constituents, with the exception of SO_4. It is also apparent that the pH and the concentration of dissolved gases are much lower. This is almost certainly due to the effects of reinjection into the nearby well RN-20b.

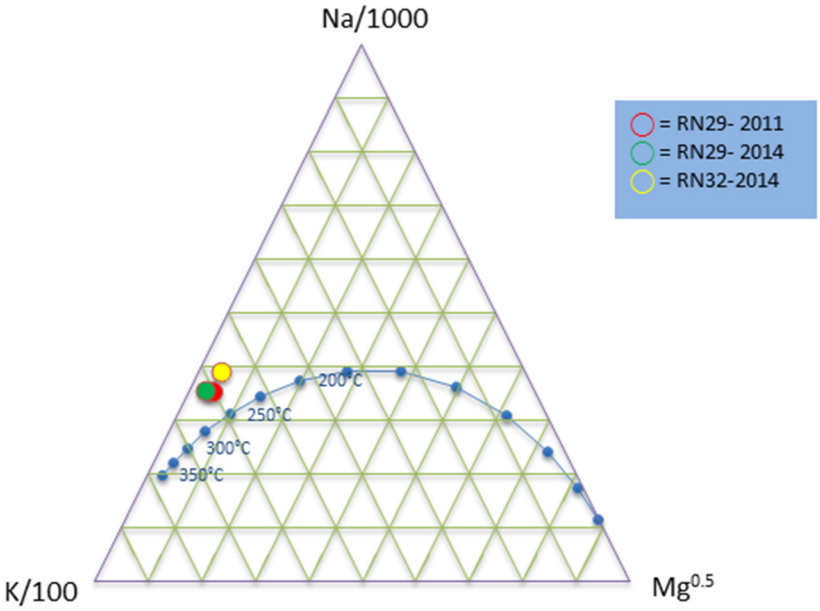

FIGURE 8: Na-K-Mg ternary diagram

TABLE 5: Aquifer water composition at reference temperatures of 290 and 250°C for wells RN-29 and RN-32, respectively; concentrations are in mg/kg

DISSOLVED SOLIDS													
Well no.	**Sample ID**	**SiO_2**	**Na**	**K**	**Ca**	**Mg**	**Cl**	**F**	**B**	**SO_4**	**Fe**	**Al**	**TDS**
RN29 2011[a]	20110005	748	9673	1688	1241	1.13	18922	0.18	7.49	16.4	0.70	0.02	32402
RN29 2011[b]	20110005	749	9674	1688	1241	0.79	1688	0.15	7.49	16.4	0.71	0.02	32405
RN29 2014[a]	20140009	860	11564	1992	1541	2.26	22607	0.21	10.30	12.8	3.02	0.02	39427
RN29 2014[b]	20140009	860	11564	1992	1541	2.26	22606	0.21	10.30	12.9	3.02	0.02	39426
RN32 2014[a]	20140137	576	9091	1321	1348	1.01	17694	0.19	7.08	24.0	0.43	0.11	30536
Sea water	Standard	5.34	10800	390	450	1290	18800	1.30	4.50	2700	0.003	0.003	33960

DISSOLVED GASES												
Well no.	**Sample ID**	**CO_2**	**H_2S**	**NH_3**	**N_2**	**O_2**	**CH_4**	**H_2**	**log(Q/K) calcite**	**log(Q/K) anhydrite**	**log(Q/K) quartz**	**Deep liquid pH**
RN29 2011[a]	20110005	1852	66.4	1.75	200	19.7	0.11	0.16	-0.555	0.109	0.129	4.7
RN29 2011[b]	20110005	1005	39.5	1.31	100	9.9	0.06	0.08	-0.193	0.201	0.093	4.9
RN29 2014[a]	20140009	2341	177.2	2.32	17.90	<0.01	0.31	1.65	-0.385	0.210	0.068	4.5
RN29 2014[b]	20140009	1190	102.0	1.97	8.39	<0.01	0.15	0.77	-0.375	0.243	0.068	4.7
RN32 2014[a]	20140137	84	3.9	1.60	3.89	<0.01	<0.01	0.03	-0.555	0.109	0.129	5.4

a = For liquid enthalpy; b = For excess enthalpy

As regards the excess enthalpy of well RN-29, the computed deep liquid concentrations, based on liquid enthalpy and excess enthalpy, show the same results in most of the dissolved solids but it is different in pH and the concentration of dissolved gases. The lower CO_2 concentration also affects the pH of the computed deep liquid.

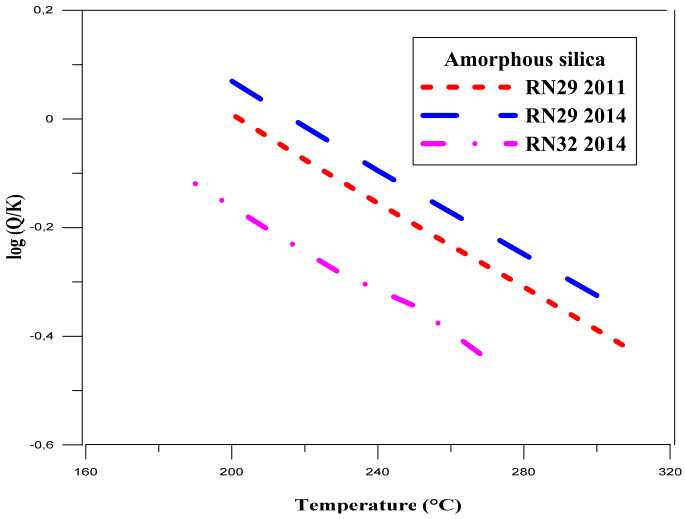

FIGURE 9: Changes in the saturation index of amorphous silica against temperature during boiling

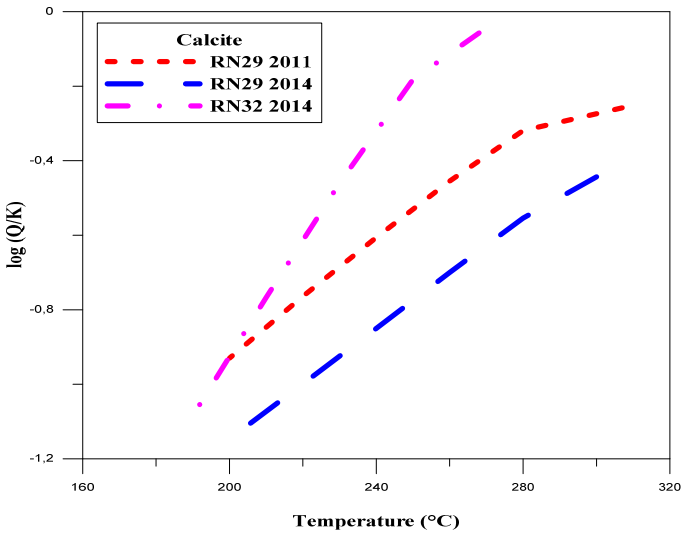

FIGURE 10: Changes in the saturation index of calcite against temperature during boiling

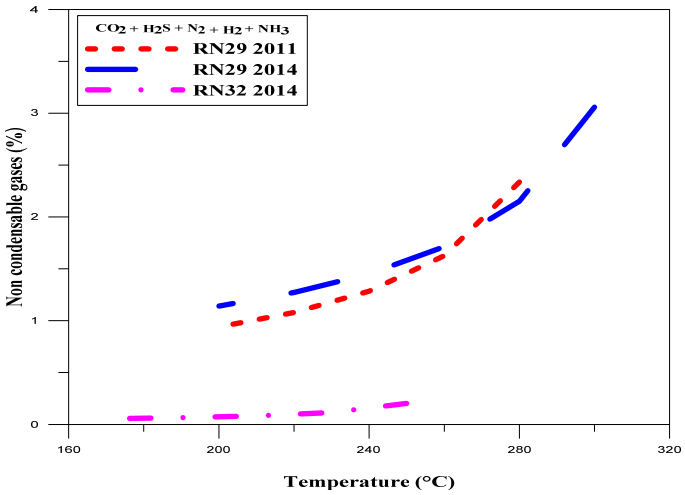

FIGURE 11: Non-condensable gas content against temperature during boiling

Also shown in Table 5 is the composition of standard seawater (Krauskopf, 1995) from which it may be seen that the deep liquid brines are very similar to seawater in terms of Na, Cl and total dissolved solids (TDS), but there are some differences in other components. These differences are mainly due to ion exchange equilibria between rock and water. When compared to seawater, the Reykjanes brine is deficient in magnesium (Mg), fluoride (F) and sulphate (SO_4) but enriched in potassium (K) and calcium (Ca). The amount of silica (SiO_2) in the geothermal brines is an order of magnitude higher than in seawater, as would be expected from its increased solubility with temperature.

5.5 Production properties

Scale deposition in production wells, pipelines and surface facilities is one of the most common problems encountered during the exploitation of geothermal systems as production of high-temperature liquid of near-seawater composition results in a pressure decrease and boiling in the wells during ascent. The boiling causes cooling and gas loss, which leads to the precipitation of base metal-rich sulphide scales (mainly sphalerite and minor chalcopyrite; Hardardóttir et al., 2009) and amorphous Fe-bearing silica, both in the well and in surface pipes. All the silicate minerals are likely to precipitate at lower temperatures. Figure 9 shows that at low temperatures (< 200°C for well RN-29, < 160°C for well RN-32) the amorphous silica starts to precipitate, and this might pose a problem in surface equipment and reinjection wells.

The deep liquid is slightly undersaturated with respect to calcite and becomes more undersaturated upon boiling, as seen in Figure 10. There should be no risk of calcite precipitation.

The non-condensable gas content (NGC) becomes lower when the temperature decreases with boiling, as the amount of vapour increases, as seen in Figure 11.

After boiling to 200°C, the NCG content in well RN-29 is about 1% (assuming liquid enthalpy), but about 0.2% in well RN-32.

5.6 Gas equilibria

The equilibrium curves of the mineral assemblages that could fix the concentrations of the reactive gases H_2, H_2S, CO_2 are plotted in Figures 12-14. In this study the dissociation reactions of the hydrothermal minerals of H_2S, H_2, and CO_2 are considered. The concentrations of H_2S, H_2, CO_2 expressed in moles per kilogram are used to plot the graph.

As seen in Figure 12, the H_2 concentration of the sample from well RN-29 in 2014 may be controlled by the gro+pyrr+qtz+epi+wol+pyr mineral assemblage but, for well RN-29 in 2011, it is difficult to decipher which of the assemblages controls H_2 concentrations.

The H_2S concentration (Figure 13) for well RN-29 in 2014 appears to be controlled by the pyr+pyrr+pre+epi mineral assemblage but, for well RN-29 in 2011, it is nearer to gro+pyr+pyrr+qtz+epi+wol. CO_2 (Figure 14) appears to be controlled by the czo+cal+qtz+gro mineral assemblage in well RN-29, both in 2011 and 2014.

The sample from well RN-32 is far from any of these mineral assemblages, probably because of mixing with reinjection water.

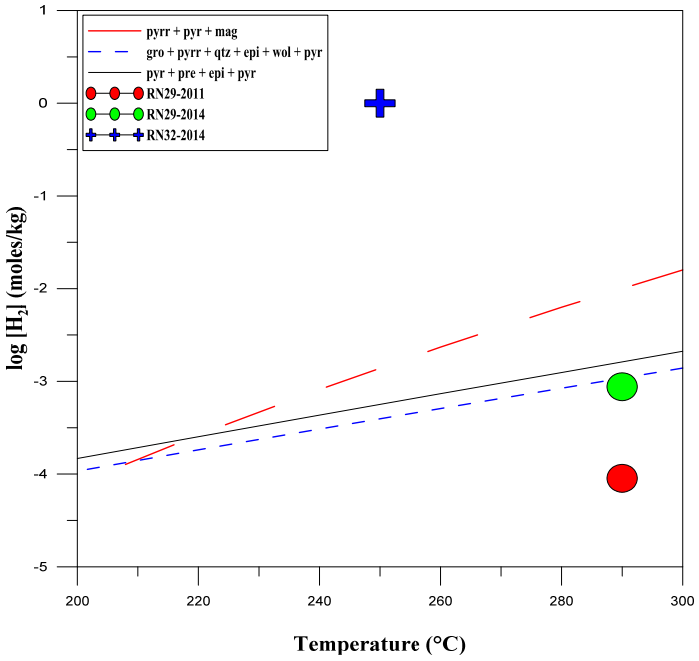

FIGURE 12: Measured concentrations of H_2 as a function of temperature, along with the mineral buffers which might control the H_2 concentration

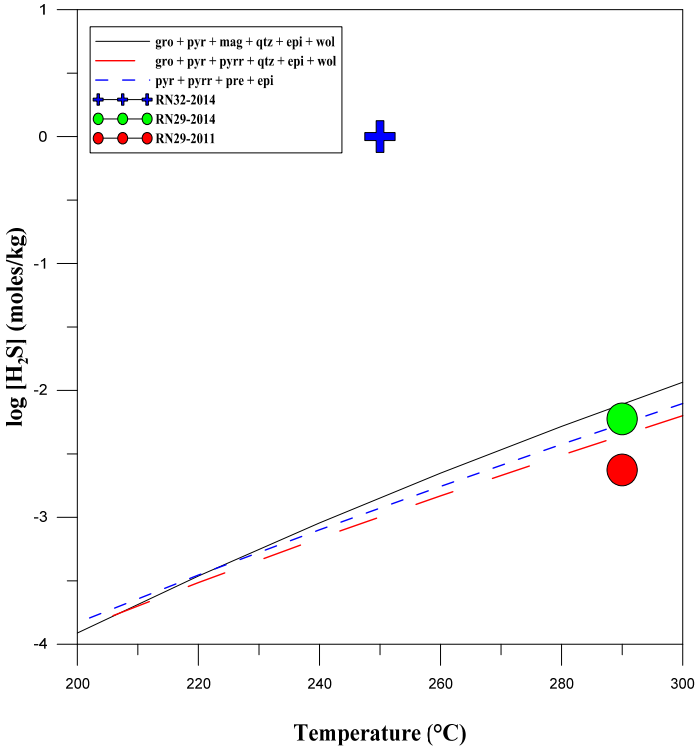

FIGURE 13: Measured concentrations of H_2S as a function of temperature, along with the mineral buffers which might control the H_2S concentration

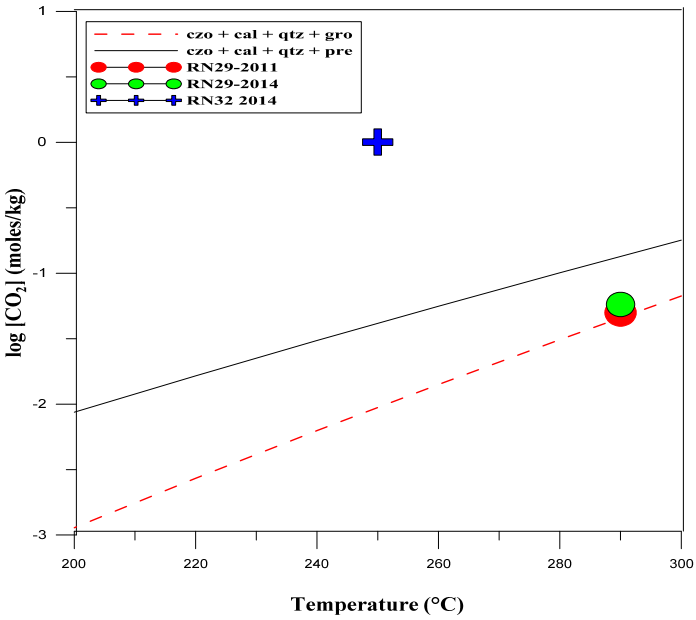

FIGURE 14: Measured concentrations of CO_2 as a function of temperature, along with the mineral buffers which might control the CO_2 concentration

6. CONCLUSIONS

Thermal waters of the Reykjanes field have Na and Cl concentrations similar to those of seawater. From geothermometers, mineral equilibria and temperature logs, it is suggested that the reservoir temperature of well RN-29 is around 290ºC and that of well RN-32 about 250°C. Well RN-29 has a measured enthalpy of 2250 kJ/Kg, higher than what corresponds to liquid enthalpy at 290°C. Various processes can cause such enthalpy of the flowing fluid; it is assumed that the excess enthalpy is caused by phase segregation in the depressurization zone around the wells. Aquifer fluid component concentrations for well RN-29 were, thus, calculated on the basis of a phase segregation model, taking the phase segregation to take place at a temperature 30°C below the aquifer temperature. The results thus obtained show significantly lower concentrations of volatile components, but there is an insignificant difference for non-volatile components. For well RN-32, liquid enthalpy was assumed when calculating the deep fluid composition. The deep liquid of well RN-32 is considerably less saline than that of well RN-29, and the concentration of dissolved gases, including CO_2 and H_2S is much lower. This is likely due to reinjection of separator fluid and condensate into nearby well RN-20b.

As the liquid boils, it becomes supersaturated with respect to amorphous silica at about 200 and 160°C for wells RN-29 and RN-32, respectively, so silica scaling is to be expected below those temperatures. Boiling should not, however, induce the precipitation of calcite. Hardardóttir et al. (2009) have, on the other hand, shown that sulphides will form upon boiling. The non-condensable gas content is rather low in well RN-29 (about 1% after boiling to 200°C), and very low in well RN-29.

ACKNOWLEDGEMENTS

I wish to thank the Government of Iceland and the United Nations University for supporting this training programme. Deepest thanks are expressed to Mr. Lúdvík S. Georgsson, director of the UNU Geothermal Training Programme and Mr. Ingimar Gudni Haraldsson, Deputy Director, for their excellent guidance and successful operation of the programme. My special thanks go to my supervisors, Mr. Finnbogi Óskarsson and Dr. Halldór Ármannsson, for their great help and critical advice during all stages of the data analysis and the preparation of this report. I wish to give my thanks to all lecturers and staff members at ÍSOR for their comprehensive presentations and willingness to share their knowledge and experience.

REFERENCES

Ármannsson, H. and Ólafsson, M., 2006: *Collection of geothermal fluids for chemical analysis*. ÍSOR – Iceland GeoSurvey, Reykjavík, report ISOR-2006/016, 17 pp.

Arnórsson, S., 1978: Major element geochemistry of the geothermal seawater at Reykjanes and Svartsengi. *Mineral Mag., 42,* 209-220.

Arnórsson, S., 1983: Chemical equilibria in Icelandic geothermal systems. Implications for chemical geothermometry investigations. *Geothermics, 12,* 119-128.

Arnórsson, S., 1989: Deposition of calcium carbonate minerals from geothermal waters-theoretical considerations. *Geothermics, 18,* 33-39.

Arnórsson, S., Angcoy, Jr., E.C., Bjarnason, J.Ö., Giroud, N., Gunnarsson, I., Kaasalainen, H., Karingithi, C., and Stefánsson, A., 2010: Gas chemistry of volcanic geothermal systems. *Proceedings of the World Geothermal Congress 2010*, Bali, Indonesia, 12 pp.

Arnórsson, S., Gunnlaugsson, E., and Svavarsson, H., 1983: The chemistry of geothermal waters in Iceland II. Mineral equilibria and independent variables controlling water compositions. *Geochim. Cosmochim. Acta*, *47*, 547-566.

Arnórsson, S., and Svavarsson, H., 1985: Application of chemical geothermometry to geothermal exploration and development. *Geoth. Res. Council, Transactions, 9-1*, 293-298.

Bjarnason, J.Ö., 2010. *The speciation program WATCH* (vers. 2.4). ISOR – Iceland GeoSurvey, Reykjavík.

Björnsson, S., Arnórsson, S., and Tómasson, J., 1970: Exploration of the Reykjanes thermal brine area, *Geothermics, Sp. issue, 2-2,* 1640-1650.

Björnsson, S., Arnórsson, S., and Tómasson, T., 1972: Economic evaluation of Reykjanes thermal brine area, Iceland. *Am. Assoc. Petr. Bull., 56-12,* 2380-2391.

Björnsson, S., Arnórsson, S., Tómasson, J., Ólafsdóttir, B., Jónsson, J., and Sigurmundsson, S.G., 1971: Reykjanes--Final Report on Exploration. Orkustofnun – National Energy Authority, report (in Icelandic), 122 pp.

Fournier, R.O., 1977: Chemical geothermometers and mixing model for geothermal systems. *Geothermics, 5,* 41-50.

Fournier, R.O., 1979: A revised equation for Na-K geothermometer. *Geoth. Res. Council, Trans., 3,* 221-224.

Fournier, R.O., 1985: The behaviour of silica in hydrothermal solutions. *Rev. Econ. Geology, 2,* 45-61.

Franzson, H., Thórdarson, S., Björnsson, G., Gudlaugsson, S.Th., Richter, B., Fridleifsson, G.Ó., and Thórhallsson, S., 2002: Reykjanes high temperature field, SW-Iceland, geology and hydrothermal alteration of well RN-10, *Proceedings of the 27th Workshop on Geothermal Reservoir Engineering,* Stanford University, Stanford, CA, 233-240.

Freedman, A.J.E., Bird, D.K., Arnórsson S., Fridriksson, Th., Elders, W.A., Fridleifsson, G.Ó., 2010: Hydrothermal mineral record CO_2 partial pressures in Reykjanes geothermal system, Iceland. *Proceedings of the World Geothermal Congress 2010, Bali, Indonesia*, 11 pp.

Fridriksson, T., Kristjánsson, B.R., Ármannsson, H., Margrétardóttir, E., Ólafsdóttir, S., and Chiodini, G., 2006: CO_2 emissions and heat flow through soil, fumaroles, and steam heated mud pools at the Reykjanes geothermal area, SW Iceland. *Applied Geochemistry, 21,* 1551–1569.

Giggenbach, W.F., 1988: Geothermal solute equilibria. Derivation of Na-K-Mg-Ca geoindicators. *Geochim. Cosmochim. Acta, 52*, 2749-2765.

Giggenbach, W.F., 1991: Chemical techniques in geothermal exploration. In: D'Amore, F. (coordinator), *Application of geochemistry in geothermal reservoir development*. UNITAR/UNDP publication, Rome, 119-144.

Gudmundsson, J.S., Hauksson, T., Tómasson, J., 1981: Subsurface exploration and well discharge characteristics, Reykjanes geothermal field in Iceland. *Proceedings of the 7th Workshop in Reservoir Engineering, Stanford University, Stanford, CA*, 61-69.

Gudmundsson, J.S. and Thórhallsson, S., 1986: The Svartsengi reservoir in Iceland. *Geothermics, 15,* 3-15.

Gunnarsdóttir, S., Stefánsson, H.Ö., Níelsson, S., Sigurgeirsson, M.A., 2013: *Well report RN-32: Drilling operations of well RN-32 from surface down to 1202 m.* ÍSOR – Iceland GeoSurvey, report ÍSOR 2013/041 (in Icelandic), 173 pp.

Hardardóttir, V., Brown, K.L., Fridriksson, Th., Hedenquist, J.W., Hannington, M.D., and Thórhallsson, S., 2009: Metals in deep liquid of the Reykjanes geothermal system, southwest Iceland: Implications for the composition of seafloor black smoker fluids. *Geology, 37/12*, 1103-1106.

Hardardóttir, V., Kristmannsdóttir, H., and Ármannsson, H., 2001: Scales formation in wells RN-9 and RN-8 in the Reykjanes geothermal field Iceland. *Proceedings of the 10th International Symposium* on *Water-Rock Interaction, Villasimius, Italy, Balkema, Rotterdam*, 851-854.

Jakobsson, S.P., Jónsson, J., and Shido, F., 1978: Petrology of the western Reykjanes Peninsula, Iceland. *J. Petrology, 19-4,* 669-705.

Johnsson, G.L., and Jakobsson, S.P., 1985: Structure and petrology of the Reykjanes Ridge between 62°55′N and 63°48′N. *J. Geophys. Res., 90-B12,* 10073-10083.

Krauskopf, K.B., 1995: *Introduction to geochemistry* (2nd ed.). McGraw Hill publ., NY, 647 pp.

Ólafsson, J., and Riley, J.P., 1978: Geochemical studies on the thermal brine from Reykjanes (Iceland). *Chemical Geology, 21*, 219-237.

Óskarsson, F., Fridriksson, Th., and Thorbjörnsson, D., 2014: Geochemical monitoring of the Reykjanes geothermal reservoir 2003 to 2013. *Submitted for World Geothermal Congress 2015, Melbourne, Australia,* 8 pp.

Pálmason, G., Johnson, G.V., Torfason, H., Saemundsson, K., Ragnars, K., Haraldsson, G.I., Halldórsson, G.K., 1985: *Geothermal assessment of Iceland*. Orkustofnun, Reykjavík, report OS-85076 /JHS-10 (in Icelandic), 176 pp.

Pope, E.C., Bird, D.K., Arnórsson, S., Fridriksson, Th., Elders, W.A., 2010: Iceland Deep Drilling Project (IDDP): Stable isotope evidence of fluid evolution in Icelandic geothermal systems. *Proceedings of the World Geothermal Congress 2010, Bali, Indonesia*, 7 pp.

Sveinbjörnsdóttir, Á.E., Coleman, M.L., and Yardley, B.W.D., 1986: Origin and history of hydrothermal fluids of the Reykjanes and Krafla geothermal fields, Iceland. A stable isotope study. *Contrib. Mineral. Petrol. 94,* 99-109.